International Journal of Nanoscience and Nanoengineering
2014; 1(2): 22-33
Published online October 30, 2014 (http://www.openscienceonline.com/journal/nano)

Tin dioxide nanostructure using rapid thermal oxidation method and hydrothermal synthesis of CuO-SnO_2-ZnO Nano composite oxides

Marwa Abdul Muhsien Hassan[1], Evan Tareq Salem[2], Nadheer Jassim Mohammed[1], Ibrahim Ramdan Agool[1]

[1]Department of Physics, College of Science, Al- Mustansiriyah University, Baghdad, Iraq
[2]School of Applied Sciences, University of Technology, Laser and Optoelectronic Branch, Baghdad, Iraq

Email address

marwa_alganaby@yahoo.com (M. A. M. Hassan)

To cite this article

Marwa Abdul Muhsien Hassan, Evan Tareq Salem, Nadheer Jassim Mohammed, Ibrahim Ramdan Agool. Tin Dioxide Nanostructure Using Rapid Thermal Oxidation Method and Hydrothermal Synthesis of CuO-SnO_2-ZnO Nano Composite Oxides. *International Journal of Nanoscience and Nanoengineering*. Vol. 1, No. 2, 2014, pp. 22-33.

Abstract

Tin dioxide (SnO_2) nanostructured thin films on quartz substrates were prepared by rapid thermal oxidation technique for different oxidation temperatures and oxidation times. X-ray diffraction analysis indicates that the films are polycrystalline, having tetragonal structure. All the films shown most preferred orientation along (101) plane parallel to the substrates. The nanostructure parameters such as grain size, microstrain and dislocation density were calculated. The grain size of prepared SnO_2 nanostructure films is small and is within the range of 44 to 56 nm. The nanocomposite oxides (CuO-SnO_2-ZnO) prepared to use hydrothermal method consist of small nanorod distributed on the surface that shows nanostructure properties.

Keywords

SnO_2 Polycrystalline Film, Rapid Thermal Oxidation, Structural Properties, Grain Size, Hydrothermal Method

1. Introduction

Tin dioxide (SnO_2) with the rutile structure is an *n*-type semiconductor with a wide band gap ~3.6 eV. The structural characteristics of polycrystalline tin oxide thin films are of great importance in various applications such as chemical sensors, solar cells, and optoelectronic devices [1, 2]. SnO_2 thin films have been fabricated using different techniques including dc gas discharge activating reaction evaporation technique [3], electron beam evaporation [4], rf sputtering [5-7], Plasma Enhanced Chemical Vapor Deposition [8], hydrothermal [9] and chemical vapor deposition [1, 10, 11]. One of the major challenges in synthesizing SnO_2 thin films is the control over stoichiometry. Since most depositions are carried out in high vacuum condition at high temperatures, the SnO_2 films obtained are nonstoichiometric and frequently consist of metastable phases such as SnO and Sn_3O_4 [12]. The existence of these metastable phases and crystal defects will strongly affect the properties of the films [12, 13]. Therefore, a post deposition annealing in the air is necessary to obtain the stoichiometric SnO_2 phase with the rutile structure. However, the microstructure of the resulting SnO_2 films is mainly controlled by the annealing process and a number of crystal defects are frequently observed in these films. The structure of the SnO_2 material in its bulk form is tetragonal rutile with lattice parameters $a = b = 4.737$ Å and $c = 3.816$ Å. However in thin film form, depending on the deposition technique its structure can be polycrystalline or amorphous. The grain size is typically 200–400 Å, which is highly dependent on deposition technique, temperature, doping level etc. SnO_2 films close to stoichiometric condition have low free carrier concentration and high resistivity, but non-stoichiometric SnO_2 films have high carrier concentration, conductivity and transparency. This comes about from an oxygen vacancy in the structure so that the formula for the thin film material is $SnO_2{-}x$, where x is the

deviation from stoichiometry [14].

In this work, we have investigated the x-ray diffraction properties of SnO_2 films prepared onto quartz substrates using rapid thermal oxidation at different oxidation temperatures and oxidation time.

2. Materials and Method

The thermal evaporation system (Edwards) has been used to evaporate the high purity (99.9 %) tin on quartz slides under low pressure (about10^{-6}torr). SnO_2 film was obtained with the aid of rapid thermal oxidation system with halogen lamp as oxidation source. The optimum oxidation condition used to form SnO_2 film was 600 ^oC and 90 sec oxidation time. Ohmic contacts were fabricated by evaporating 99.999 purity aluminum wires in a tungsten boat. In order to explain the structural properties of films prepared at different conditions, X-ray diffraction measurement was carried out according to the ASTM (American Society of Testing Materials) cards, using Philips pw 1050 X-ray diffractometer of 1.54056 Å from Cu-kα. The topography of the SnO_2 thin films prepared under various preparation conditions were investigated with an optical microscope (500X magnification power type Nikon ECLIPSE ME600). A digital Camera (DXM1200F) and a computer was added to store the surface image of the prepared films.

2.1. Hydrothermal Synthesis of (MOS)Nano-Composite Oxides

Metal oxide semiconductor nanocomposite prepared by using ($Cu(NO_3)_2.3H_2O$ (0.07 mol), $Zn(NO_3)_2.6H_2O$ (0.07 mol) and $SnCl_2.2H_2O$ (0.07 mol)) were initially dissolved in 250 ml of water, ethanol and HCl. Then urea (0.2 mol) was added to the homogeneous liqude and transferred into a Teflon lined stainless steel autoclave with a volume of 50 ml, the autoclave was sealed and kept at 180 C° for 10 hour on hot plate stirrer with slow stirring. After the complete reaction, it was cooled to 35°C (room temperature). The product was filtered, washed with water, acetone and dried at 120 °C in oven (hot air). The prepared nanocomposite were examined by X-Ray diffraction (miniflex II Rigaku, Japan) (Cu, kα), Atomic Force Microscope (AFM) to study the morphology of the nanocomposite surface and Field Emission Scanning Electron Microscope (Hitachi S-4160) (FESEM) to study the structural properties of the nanocomposite.

3. Results and Discussion

3.1. X –Ray Diffraction

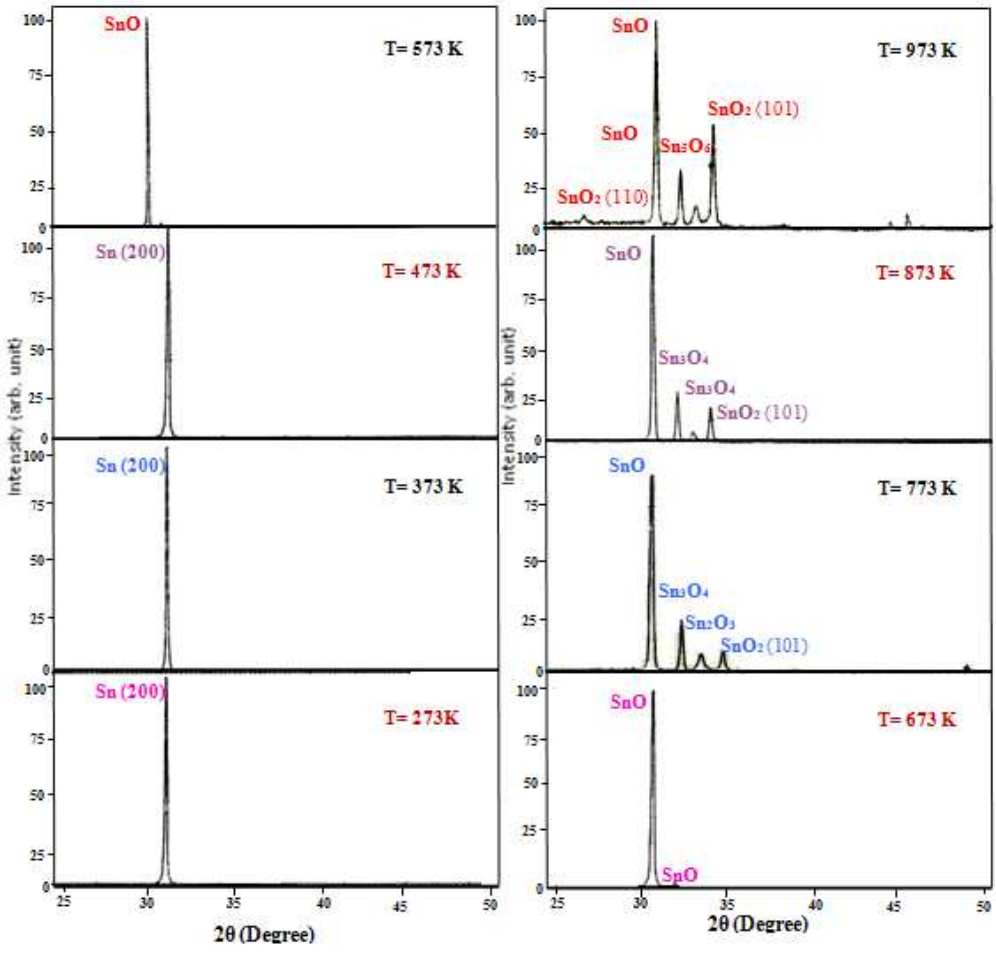

Figure 1(a). *X-Ray diffraction patterns for SnO_2 thin films prepared at different oxidation temperature and 60 sec.*

The crystallinity of the produced material was characterized using x-ray diffraction (XRD). This technique was also employed by other group which gives an indication about the grain size and formation material type of the prepared thin film. The following figures show the XRD patterns for samples grown at different oxidation temperature and oxidation time. For Sn films depositing on quartz substrate. One peak could be recognized in figure (1) (a), film is single crystalline with a tetragonal structure according to the ASTM standards where (200) Sn, with lattice constant of (a=5.8285 Å) respectively could be recognized. This is related to the formation of tin thin film and such result indicates that no formation of the oxide film occurs on quartz substrate. Figure (1) (a) represents the sample prepared at 373K and 473 K oxidation temperatures and constant oxidation time. There is one sharp peak in this pattern at 2θ =30.64° for Sn film correspond to diffraction from (200) plane, where no formation of the oxide film and all the lines correspond to a single crystalline tetragonal Sn phase. At further increase in oxidation temperature up to 573 and 673 K, figure (1) (a), the XRD pattern consists of two sharp peaks at 2θ= 30.13° and 2θ=30.76° which is related to the formation of SnO film with orthorhombic structure. The intensities of the ( ) and (101) peaks show the formation of SnO oxide and a polycrystalline in nature. XRD results for a sample prepared at 773 and 873 K, where four peaks are recognized. In this diffraction pattern, the peaks at 2θ=33.8436° and 2θ= 34.0896° are corresponding to the diffraction from (101) plans which are related to the formation of cassiterite-SnO_2 films. The XRD pattern at the oxidation time of 60 sec and increasing temperature up to 973 K is shown in figure (1) (a). It is showing that the peaks at 2θ=26.73° and 2θ=34.06° in the spectra of the SnO_2 are corresponding to the reflection from the planes (110) and (101) , respectively. The intensities of the peaks are increasing with increases of oxidation temperature, which can be attributed to the improvement in the crystallinity at higher oxidation temperature. This improvement in the structural order can also be attributed to the increase in the SnO_2 film density, which results in demonstrated of (101) SnO_2 peak rather than other peak.

Figure (1) (b) shows the diffraction pattern for samples prepared at different oxidation time. At 90 sec oxidation time, the structures of films are clearly improved where a significant increase in peak intensity at (101) plane. This indicates the formation of nearly stoichiometry SnO_2 films. The intensities of these peaks reduce with the increasing of oxidation time up to (120 sec) as shown in figure (1) (b). The results that the optimal oxidation temperature are 873 K and oxidation time are 90 sec. The deviation in XRD peak of the film with respect to the standard ASTM data is attributed to the mechanical micro stress produced by different sources like impurities, defects and vacancies reside in the film structure. Results at higher oxidation time (140 sec) and at the same oxidation temperature are shown in figure (1) (b), which recognizes the peaks at 2θ=33.98° in the spectra of SnO_2 film corresponding to the reflection from (101) plane. The presence of sharp peak (in all deprogram) indicates that all films are polycrystalline in nature with a tetragonal structure and in accordance with data reported in literature [15-17]. Table (1) shows the effect of oxidation temperatures and oxidation times on the XRD characteristics evaluated from the diffrograms. Figure (2, 3) shows the relation between *(d)* spacing with oxidation temperature and oxidation time.

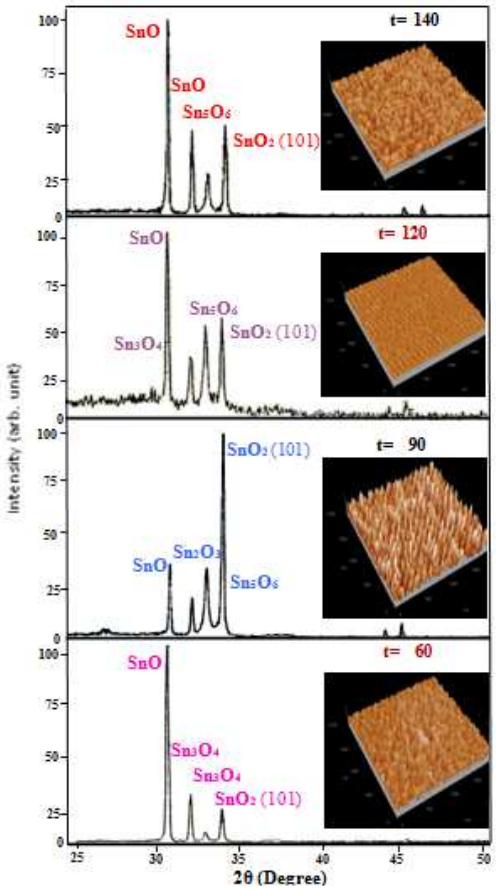

Figure 1(b). *X-Ray diffraction patterns for SnO_2 thin films prepared at 873 K for different oxidation time.*

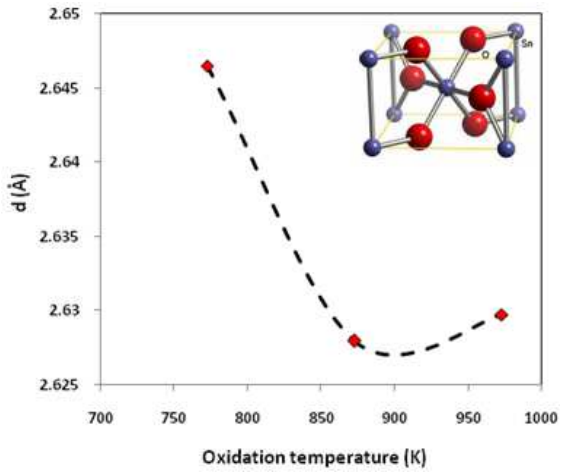

Figure 2. *Relation between d spacing and oxidation temperature of SnO_2 thin films.*

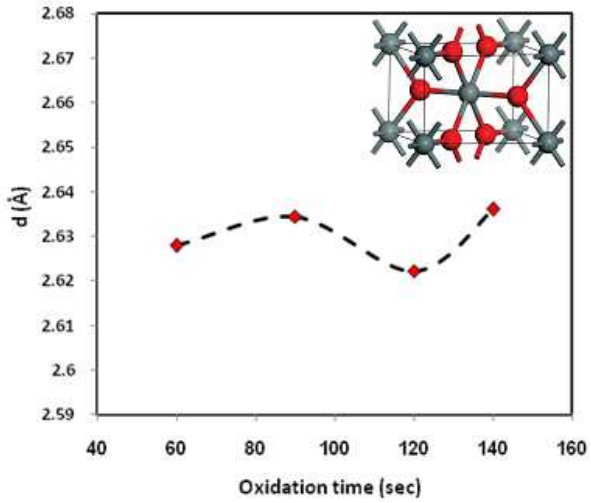

Figure 3. *Relation between d spacing and oxidation time of SnO_2 thin films.*

In the case of tetragonal structure which is the ruling form for SnO_2 thin films, the lattice constants are a=b≠ c as shown in Table (2). These constants change with structural change caused by the different parameters such as deposition technique, doping, substrate, etc., and the lattice constant can be found by measuring different values of *(d)* not less than two or three or four times of x-ray spectrum by using the formula [18]:

$$\frac{1}{d^2} = \frac{h^2 + k^2}{a^2} + \frac{l^2}{c^2} \quad (1)$$

where *h*, *k*, *l* are the Miller indices of the lattice plane. The values of lattice constants for SnO_2 films prepared at different oxidation temperature and oxidation time have been listed in Table (2). It is inferred that the lattice parameters values are in very close agreement with the standard values. Figure (4, 5) shows the dependence of the (101) plane intensity peak on oxidation temperature and oxidation time of SnO_2 thin films.

Table 1. *XRD patterns characteristics of SnO_2 films at various oxidation temperatures and oxidation times.*

Deposition condition	(2Θ)°	I/I_1 XRD	d (Å) XRD	(h k l)	(2Θ)° ASTM	I/I_1 ASTM	d (Å) ASTM	Type	ASTM Card no.
t= 60 sec T= R.T	30.6529	100	2.91429	200	30.698	100	2.91	Sn	01-0962
t= 60 sec T= 373 K	30.6402	100	2.91547	200	30.698	100	2.91	Sn	01-0962
t= 60 sec T= 473 K	30.6257	100	2.91682	200	30.698	100	2.91	Sn	01-0962
t= 60 sec T= 573 K	30.1340	100	2.96328		30.063	100	2.97	SnO	01-0891
t= 60 sec	30.7633	100	2.90408	101	30.807	80	2.90	SnO	24-1342
T= 673 K	31.0598	4	2.87703	---	30.916	90	2.89	SnO	07-0195
t= 60 sec	30.5953	100	2.91964	---	30.484	50	2.93	β-SnO	07-0195
	31.9622	22	2.79783	---	31.727	80	2.818	Sn_3O_4	16-0737
T= 773 K	32.8650	4	2.72301	030	32.964	30	2.715	Sn_2O_3	25-1259
	33.8436	16	2.64648	101	33.875	81	2.644	SnO_2	21-1250
t= 60 sec	30.8484	100	2.89626	---	30.916	90	2.89	SnO	07-0195
	32.2340	25	2.77486	---	32.315	50	2.768	Sn_3O_4	16-0737
T= 873 K	33.1044	8	2.70386	---	33.014	50	2.711	Sn_3O_4	16-0737
	34.0896	10	2.62794	101	34.061	80	2.63	SnO_2	02-1340
t=90 sec	30.7698	31	2.90348	101	30.807	80	2.90	SnO	24-1342
	32.7901	6	2.72906	030	32.964	30	2.715	Sn_2O_3	25-1259
T= 873 K	33.0188	30	2.71068	---	33.026	30	2.7100	Sn_5O_6	18-1386
	34.0027	100	2.63446	101	34.061	80	2.63	SnO_2	02-1340
t=120 sec	30.9004	100	2.89151	---	30.916	90	2.89	SnO	07-0195
	32.3045	26	2.76896	---	32.315	50	2.768	Sn_3O_4	16-0737
T= 873 K	33.1776	42	2.69806	---	33.026	30	2.7100	Sn_5O_6	18-1386
	34.1664	45	2.62221	101	34.195	80	2.62	SnO_2	03-0439
t=140 sec	30.7550	100	2.90485	101	30.807	80	2.90	SnO	24-1342
	32.1293	40	2.78366	021	32.172	40	2.78	SnO	24-1342
T= 873 K	33.0054	18	2.71175	---	33.026	30	2.7100	Sn_5O_6	18-1386
	33.9813	46	2.63607	101	33-928	63	2.64	SnO_2	01-0657
	26.7397	4	3.33123	110	26.749	80	3.33	SnO_2	02-1340
t= 60 sec	30.8386	100	2.89716	---	30.916	90	2.89	SnO	07-0195
T= 973 K	32.2104	26	2.77684	021	32.172	40	2.78	SnO	24-1342
	33.0762	9	2.70610	---	33.026	30	2.7100	Sn_5O_6	18-1386
	34.0658	50	2.62972	101	34.061	80	2.63	SnO_2	02-1340

Table 2. *Lattice constants as a function of oxidation temperature and oxidation time of SnO_2 thin film.*

Deposition condition	investigated line	Type	Lattice (a) Å	Lattice (c) Å
t=60 sec, T= 773 K	101	SnO_2	4.739	3.190
t=60 sec, T= 873 K	101	SnO_2	4.706	3.168
t=90 sec, T= 873 K	101	SnO_2	4.717	3.175
t=120 sec, T= 873 K	101	SnO_2	4.695	3.161
t=140 sec, T= 873 K	101	SnO_2	4.720	3.177
t=60 sec, T= 973 K	101	SnO_2	4.709	3.170
ASTM	101	SnO_2	4.750	3.198

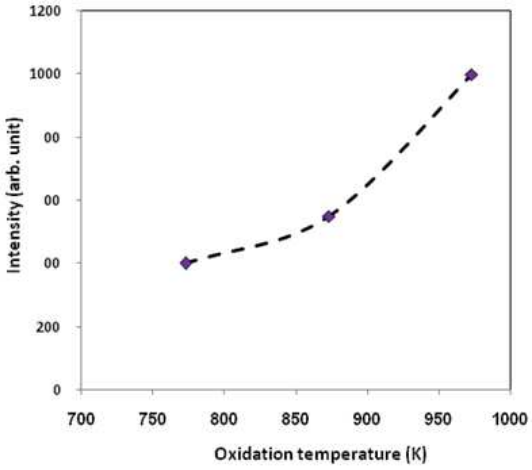

Figure 4. *Effect of oxidation temperature on the relative intensity of investigated peak (101).*

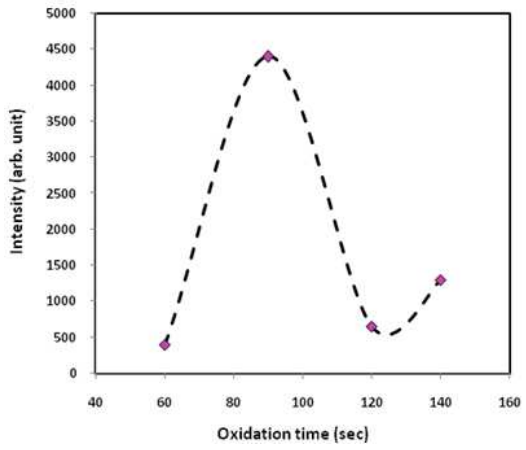

Figure 5. *Effect of oxidation time on the relative intensity of investigated peak (101).*

The FWHM of the preferred orientation (peak) could be measured, since it is equal to the width of the line profile (in degrees) at the half of the maximum intensity.The results obtained from XRD show that the FWHM of SnO_2 films are reduced at optimum condition (873 K, 90 sec), which meansthat the grain size and crystallite of the SnO_2 films are increased. The result is listed in Table (3) for all samples prepared at different oxidation temperature and oxidation time. Figure (6, 7) shows the effect of oxidation temperature and oxidation time on FWHM of SnO_2 thin films.

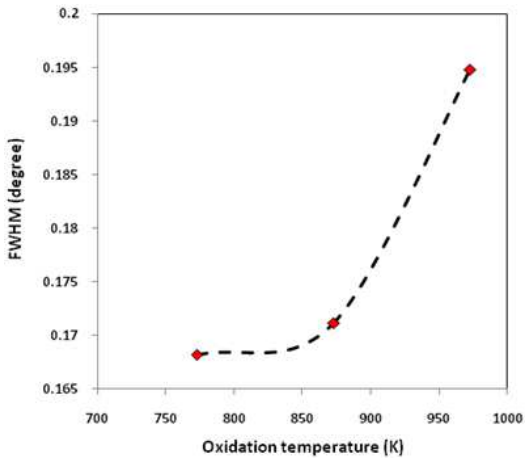

Figure 6. *The relation between oxidation temperature and structure FWHM.*

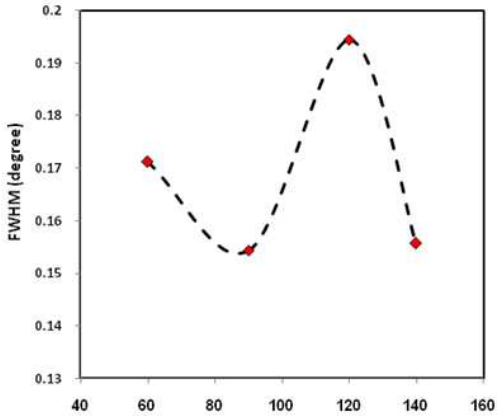

Figure 7. *The relation between oxidation time and structure FWHM.*

The grain size (D) is calculated using the Scherer formula from the full-width half-maximum (FWHM) (β) [19]:

$$D=k\lambda/\beta\cos\theta \quad (2)$$

where λ is the wavelength of the X-ray used, β is the FWHM, D is the grain size value and θ is half the angle between incident and the scattered X-ray beams. The (D) values listed in the Table 3. It shows that grain size of the films is increased with increasing of oxidation time up to (90 sec).

The intense and sharp peaks in XRD pattern reveal the good crystallinity of the films and also confirm the stoichiometric nature of SnO_2 films as shown in figure (8, 9).

Assumes the world Warren that the mathematical representation of curves resulting from the X-ray diffraction (XRD) depends primarily on the amount of similarity between these curves and functions of each of the Cauchy and Gauss, In the case considered curve X-ray diffraction is similar to function Cauchy and take the form of $(1+k^2x^2)^{-1}$, the correction is given by the following relationship, which was called (Scherer's correction):

$$\beta_{cs} = \beta_m - \beta_i \quad (3)$$

Compensation equation (3) in the relationship (2) we get:

$$D = K\lambda/[(\beta_m - \beta_i)\cos(\theta)] \quad (4)$$

In the case considered X-ray diffraction curve similar to the Gauss function which takes the form exp ($-k^2x^2$) the accuracy to be higher because of the great similarity between this function and the diffraction curves; it was suggested (Warren) correction form:

$$\beta_{cs}^2 = \beta_m^2 - \beta_i^2 \quad (5)$$

This correction called (Warren's Correction)

Compensation (5) in the relationship (2) we get:

$$D = K\lambda/[(\beta_m^2 - \beta_i^2)^{1/2}\cos(\theta)] \quad (6)$$

Since the output line shape does not resemble the Gauss curve and Cauchy curve completely, so these relations have limited operation values. If the intensity curve does not sharp may be used (Scherer's correction) or (Warren's Correction) former because the difference between the values given by relations (4) and (6) is not large, which means that the decrease of the curve breadth (an increase of sharpness) means that the effect of the amount (β_i) is significant, since the width of the curve in the half intensity (FWHM) is inversely proportional with grain size according to equation (2), the decrease in (FWHM) leads to increase in the grain size, which means that few crystal defects are present in the sample.

Moreover, Warren was suggested a relationship takes into account the geometric meaning which is [20, 21]:

$$\beta_{cs} = [(\beta_m - \beta_i)(\beta_m^2 - \beta_i^2)^{1/2}]^{1/2} \quad (7)$$

Compensation (7) in the relationship (2) we get:

$$D = K\lambda/[[(\beta_m - \beta_i)(\beta_m^2 - \beta_i^2)^{1/2}]^{1/2}\cos(\theta)] \quad (8)$$

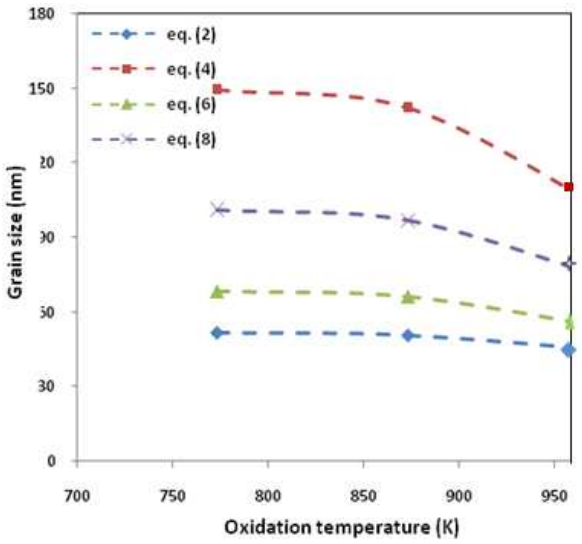

Figure 8. *Grain size as a function of oxidation temperature for SnO_2 thin films.*

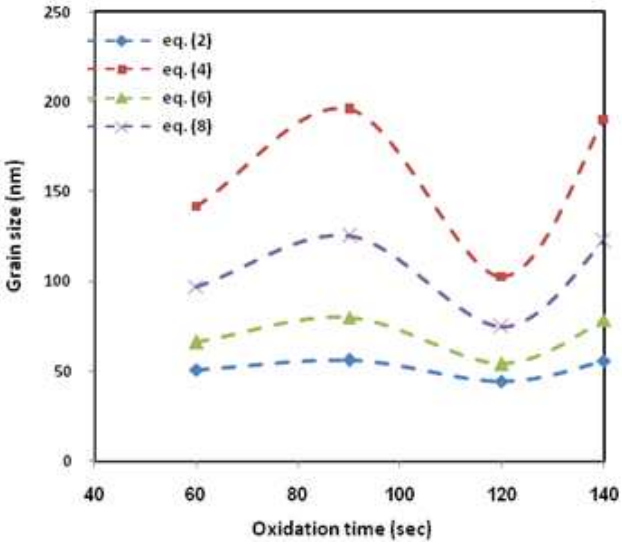

Figure 9. *Grain size as a function of oxidation time for SnO_2 thin films.*

Table 3. *Grain size of SnO_2 Thin Film.*

Deposition condition	investigated line	TYPE	β (degree)	Grain Size (D) nm eq.(2)	Grain Size (D) nm eq. (4)	Grain Size (D) nm eq. (6)	Grain Size (D) nm eq. (8)
t=60 sec, T= 773 K	101	SnO_2	0.1682	51.5877	149.0902	68.1918	100.8302
t=60 sec, T= 873 K	101	SnO_2	0.1712	50.7169	141.8748	66.18714	96.9035
t=90 sec, T= 873 K	101	SnO_2	0.1544	56.2223	195.5119	80.11873	125.1566
t=120 sec, T= 873 K	101	SnO_2	0.1945	44.6505	102.7755	54.14076	74.5945
t=140 sec, T= 873 K	101	SnO_2	0.1557	55.7497	189.9394	78.77304	122.3197
t=60 sec, T= 973 K	101	SnO_2	0.1948	44.5697	102.3843	54.0037	74.3581

The dislocation density (δ) has been calculated by using the following formula [22], for SnO_2 thin films:

$$\delta = 1/D^2 \quad (9)$$

The dislocation density for SnO_2 film is increased with increasing of oxidation temperatures, and they decreased with increasing of oxidation times. It appears clearly from the results that these are an enhancement in the film structure and homogeneous with increasing of oxidation time up to (90 sec). Figure (10, 11) shows the effect of vibration oxidation temperature and oxidation time on the value of dislocation density.

The strain values (ε) can be evaluated by using the following relation [22]:

$$\varepsilon = [\lambda / D \sin(\theta)] - [\beta / \tan(\theta)] \quad (10)$$

It can be generally observed that strain and dislocation density of the film decreases as the particle size increases

which is a well-known phenomenon [23]. Strain is inherent and natural component of SnO_2 materials as shown in figure (12, 13). Due to the large number of grain boundaries and the concomitant short distance between them. Moreover, the increasing surface energy contributes to the varying magnitude of strain.

Table 4. *Structural parameters of SnO_2 Thin Film.*

Deposition condition	Grain Size (D) nm eq. (8)	investigated line	Type	Maximum Intensity(I_{max}) (Arb. Unit)	Micro strain (ε) $x10^{-2}$	Dislocation density (δ) $x10^{10}$ lines/cm^2	Integral breadth (Δ)degree	Shape factor (Φ)
t=60 sec,T= 773 K	100.8302	101	SnO_2	400	4.30	0.98	1.68	0.10
t=60 sec, T= 873 K	96.9035	101	SnO_2	550	4.48	1.06	1.52	0.11
t=90 sec, T= 873 K	125.1566	101	SnO_2	4400	3.36	0.63	0.35	0.44
t=120 sec,T= 873 K	74.5945	101	SnO_2	950	5.96	1.8	1.87	0.10
t=140 sec,T= 873 K	122.3197	101	SnO_2	1200	3.43	0.66	0.64	0.24
t=60 sec, T= 973 K	74.3581	101	SnO_2	1000	6.00	1.81	1.93	0.10

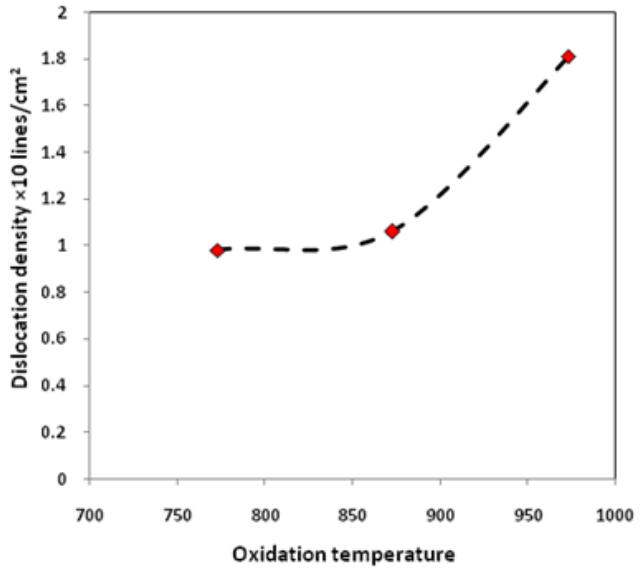

Figure 10. *Dislocation density as a function of oxidation temperature for SnO_2 thin films.*

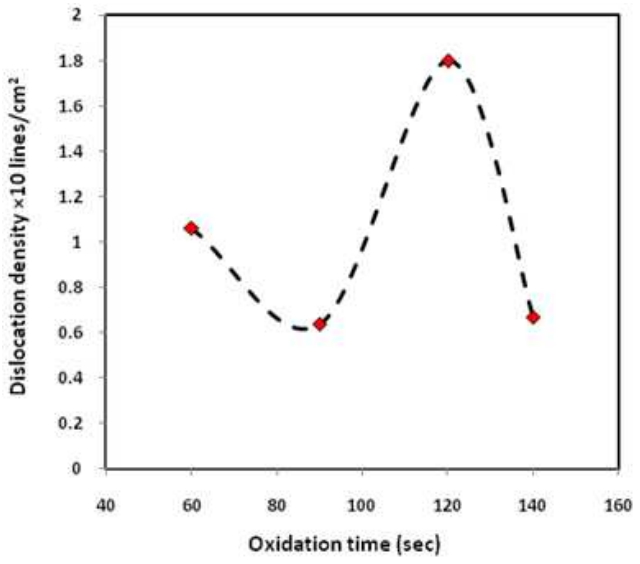

Figure 11. *Dislocation density as a function of oxidation time for SnO_2 thin films.*

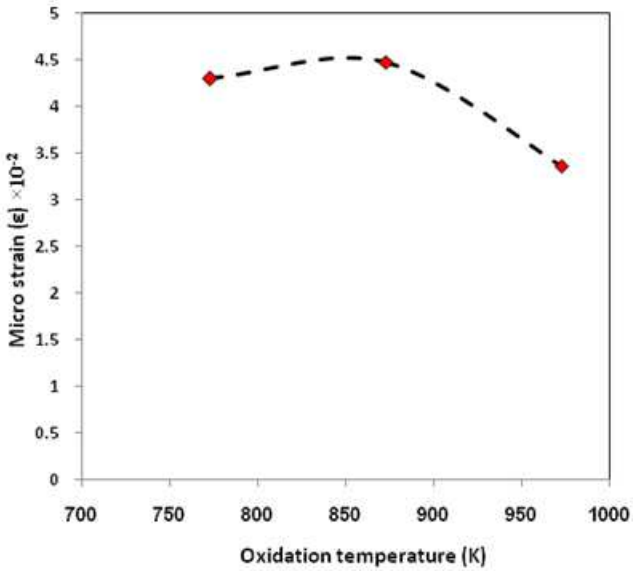

Figure 12. *Micro strain as a function of oxidation temperature for SnO_2 thin films.*

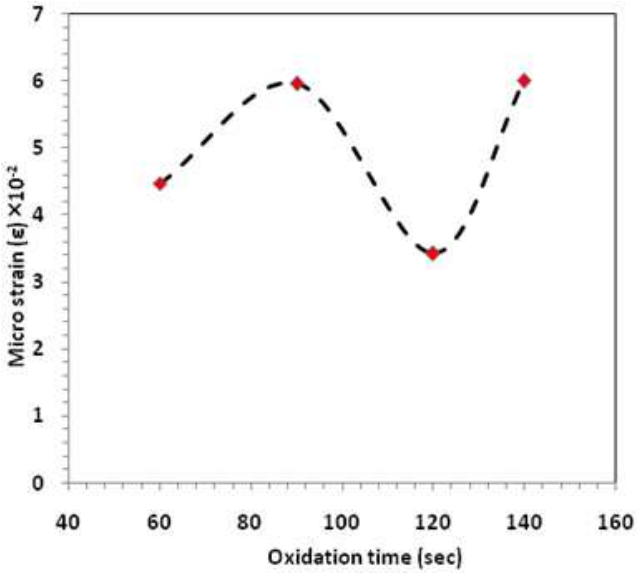

Figure 13. *Micro strain as a function of oxidation time for SnO_2 thin films.*

3.2. Integral Breadth (Δ)

There are two branches of line profile analysis:

1 Broadening.

2 Shape of diffraction line.

The first one is caused by non ideal optics of the instrument , wavelength , dispersion and structural imperfections of the specimen , also this branch is subdivided into size broadening (which is caused by the finite size of domains), and strain broadening (which is caused by varying displacements of the atoms with respect to their reference–lattice positions) . The second is frequently characterized by means of one or two breadth measures FWHM, and Δ which is given by [24]:

$$\Delta = Area/I_{max} \quad (11)$$

where:

Area = area under peak.

I_{max} = maximum intensity.

The integral breadth of the samples were obtained from the XRD pattern sheets and using the relation (11) , our results indicate that increasing the oxidation temperature leads to increasing in the integral breadth , they are recorded in the table (4) above .

The shape factor of the line profile resulting from the XRD patterns could be calculated from the relation [24]:

$$\varphi = \beta / \Delta \quad (12)$$

The shape factor was calculated using the relation (12), the results show that the shape factor had decreased with increasing of oxidation temperatures, and they increased with increasing of oxidation times.

All these parameters are calculated and presented in Table 4.

3.3. Surface Morphology

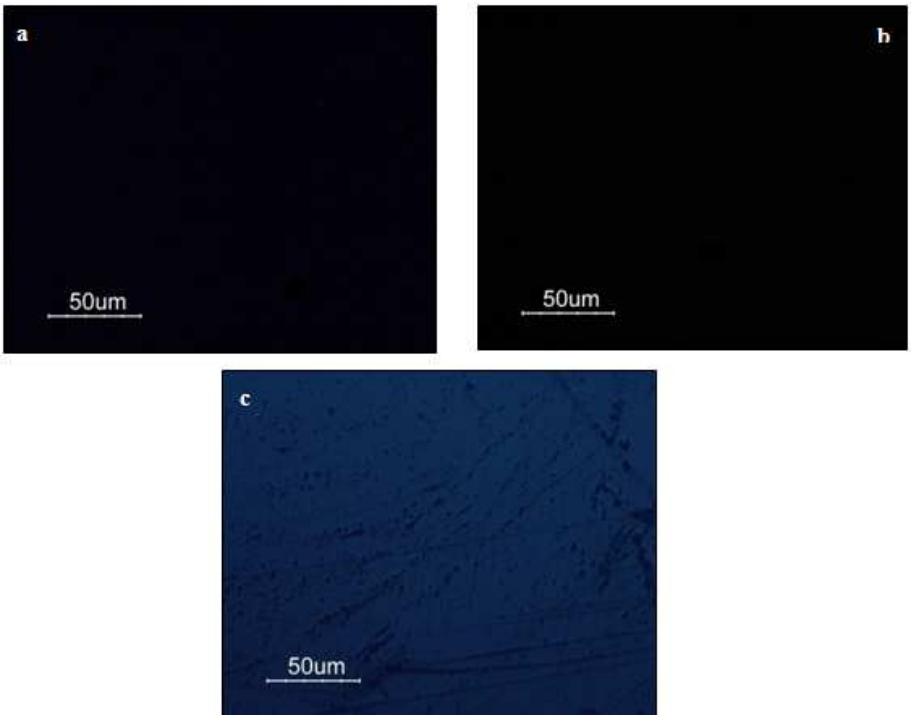

Figure 14. *Surface morphology of Sn samples prepared on quartz substrate (a) at room temperature (b) oxidation temperature (373 K) at oxidation time 60 sec and (c) oxidation temperature (473 K) at oxidation time 60 sec*

We have studied the surface morphology of the produced TCO films. The following figures show the optical micrograph of SnO_2 thin films, those prepared at various growth conditions. These micrographs reveal that the film morphology can be easily recognized through the film homogeneity and color.

Figure (14), gives the optical micrographs of the 250 nm films thickness deposited on quartz substrate and oxidized at different oxidation temperature and constant oxidation time. The color of films tends to be dark (nearly black) which reflect the metallic nature of Sn, which typically has dark color as well as the high reflectivity of the obtained film. It can clearly be noticed that the film color is the same as the physical color of the thin metal, so, they look in dark black (a, b) and less darkness obtain at 473 K in figure (c) where the transformation films to oxide films started.

The optical micrographs at an oxidation time of 60 sec and oxidation temperature of 573 and 673 K are shown in figures (15) (a, b), also recognized changes in the prepared film and morphology changes to become more transparent and less darkness in relation to transmission of microscope light through the prepared film. In the last figure, the dark droplets and particles of submicron sizes are observed over the film surface and they are spread randomly as dark regions on the film surface which results from incomplete transformation of Sn film to its oxide.

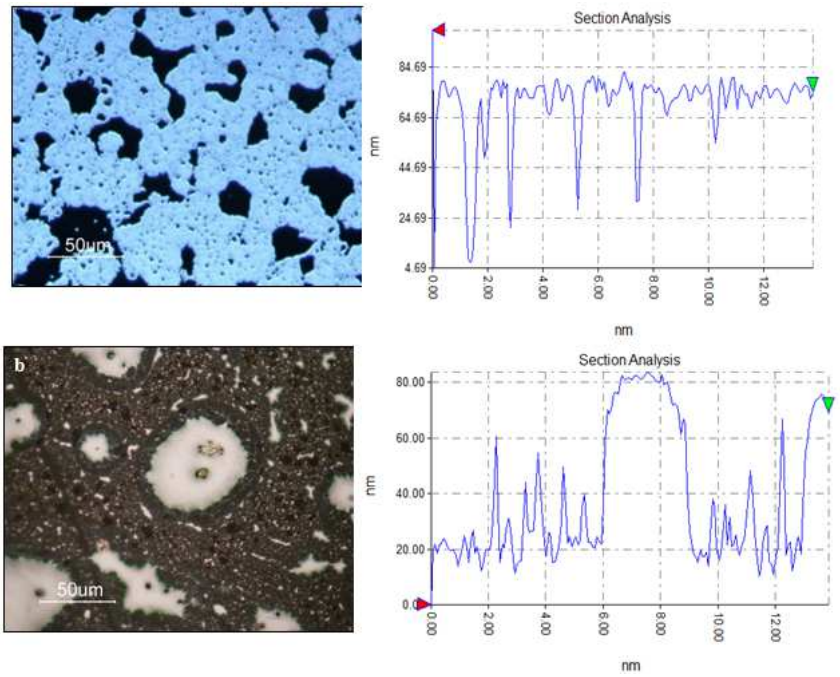

Figure 15. *Surface morphology of (SnO) samples prepared at oxidation time 60 sec (a) oxidation temperature (573 K) and (b) oxidation temperature (673 K)*

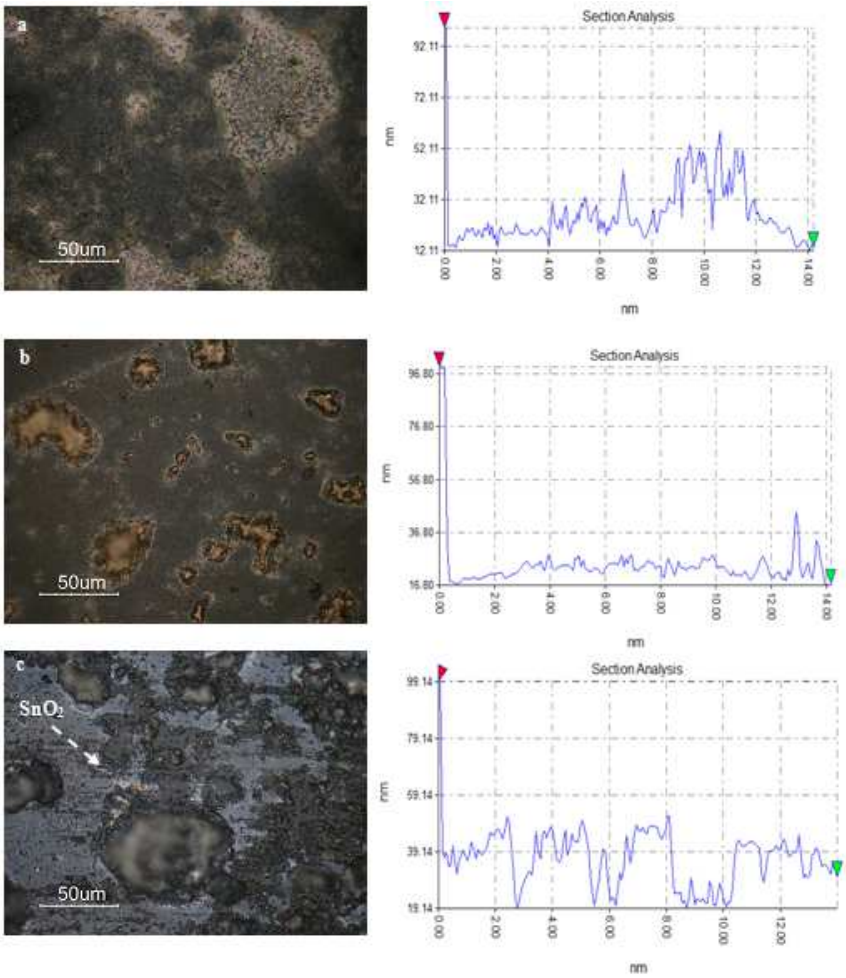

Figure 16. *Surface morphology of (SnO_2) samples prepared at oxidation time 60 sec (a) oxidation temperature (773 K), (b) oxidation temperature (873 K) and (c) oxidation temperature (873 K).*

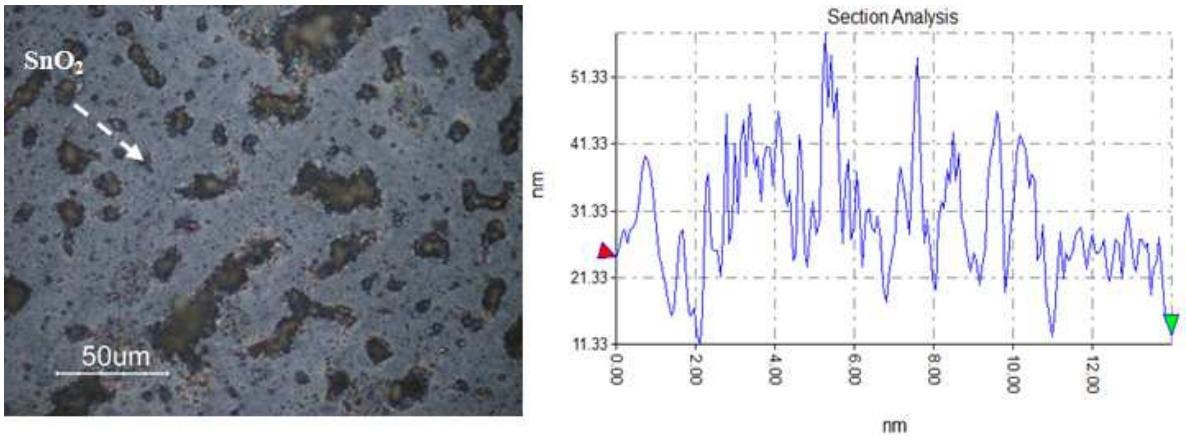

Figure 17. *Surface morphology of (SnO_2) samples prepared at oxidation temperature (873 K) and oxidation time (90 sec)*

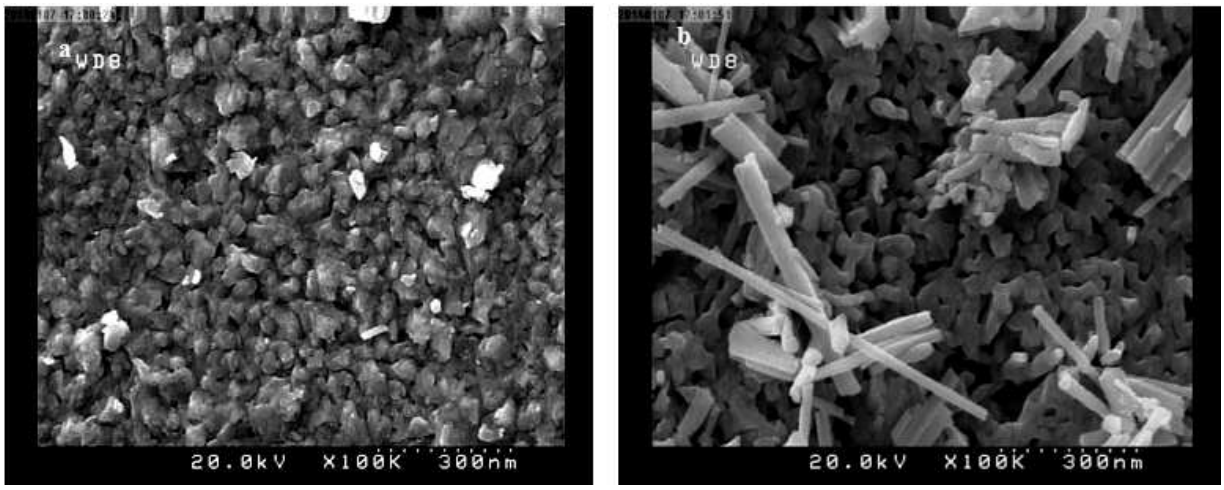

Figure 18. *FESEM image of (a) SnO_2 and (b) nanocomposite oxide CuO-SnO_2-ZnO*

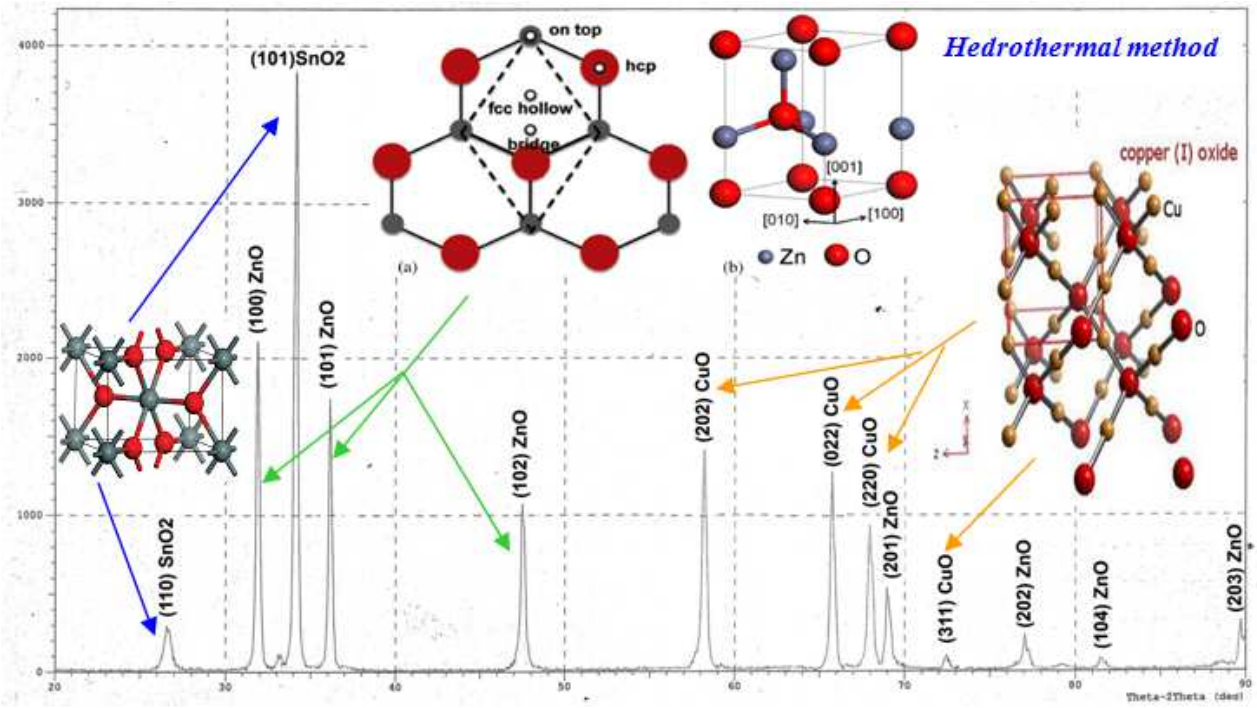

Figure 19. *XRD pattern of nanocomposite oxide CuO-SnO_2-ZnO*

At higher oxidation temperature around 773 and 873 K, figures (16) (a, b) shows that oxides film begins to demonstrate over the metal atoms that are still available in the film structure which reflects the incident light, so they appear as black dots in the microscope picture. While the oxides appear as brown particles for tin oxide molecules respectively. This result is inconsistent with XRD result which will be given later. The obtained films at oxidation temperature of 973 K for Sn film figure (16) (c) display very smooth uniform grain size and void-free film. The best surface morphology of produced films which represents the optimum case was obtained at 873 K oxidation temperature and oxidation time of 90 sec in figure (17) where Sn metal film totally transform to its SnO_2 film.

Surface morphologies obtained through SEM study carried out by (Hitachi FE-SEM model S-4160, Japan) in University of Tehran at 20 kV of CuO-SnO_2 –ZnO mixed oxide prepared using hydrothermal method. SEM micrograph shows that surface of SnO_2 oxide is smoother as shown in Figure (18) (a). The mixed oxides consist of small nanorod distributed on the surface that shows nanostructure properties. The structure is polycrystalline with very fine pores distributed fairly uniformly on the surface.

Figure (19) shows the X-ray diffraction (XRD) pattern of the CuO-SnO_2–ZnO nanocomposite oxide prepared using hydrothermal method. There are two peaks with 2θ values of 26.7^o and 34.1^o corresponding to SnO_2 crystal planes peaks of (110), (101) and show four peaks corresponding to CuO at planes of (202), (022), (220) and (311) respectively. X– ray diffraction spectra possess recognized four sharp and three small peaks for zinc oxide. It means that the ZnO is polycrystalline with crystal planes (100), (101), (102) and (201).

4. Conclusion

SnO_2 thin films were prepared onto quartz substrate by rapid thermal oxidation technique at different oxidation temperature and oxidation time. The structures of the films consist of fine (44-56 nm grain size) highly oriented grains with tetragonal (101) planes. The grain size increases when the oxidation time increases. All the films prepared at different oxidation temperature and oxidation time shows tetragonal structure. The nanocomposite oxides (CuO-SnO_2-ZnO) prepared using hydrothermal method consist of small nanorod distributed on the surface that shows nanostructure properties.

References

[1] T. J. Stanimirova, P. A. Atanasov, I. G. Dimitrov, A. O. Dikovska" Investigation on the structural and optical properties of tin oxide films grown by pulsed laser deposition" Journal of Optoelectronics and Advanced Materials, Vol. 7, No. 3, June (2005), pp: 1335 – 1340.

[2] Novinrooz, Abdoljavad; Sarabadani, Parvin; Garousi, Javad "Characterization of Pure and Antimony Doped SnO_2 Thin Films Prepared by the Sol-Gel Technique" Iran. J. Chem. Chem. Eng. Vol. 25, No.2, (2006), PP: 31-38.

[3] Shengyue Wang, Wei Wang, Qingxiang Hu, Yitai Qian, "Surface modification of tin oxide ultrafine particle thin films", Materials Research Bulletin, Vol. 35, (2000), pp: 1235–1241.

[4] Sardar M. Ayub Durrani "Biasing Voltage Dependence of Sensitivity of Electron Beam Evaporated SnO_2 Thin Film CO Sensor" Sensors, Vol.6, (2006), pp: 1153-1160.

[5] K. Zakrzewskaa, M. Radeckaa, J. Przewoz´nika, K. Kowalskia, P. Czuba "Microstructure and photoelectrochemical characterization of the TiO_2–SnO_2 system" Thin Solid Films, 490, (2005), pp: 101 – 107.

[6] Young-ll Kim, Joo-Byoung Yoon, Jin-Ho Choy, Guy Campet, Didier Camino, Josik Portier, and Jean Salardenne" Rf sputtered SnO_2, Sn-doped In_2O_3 and Ce-doped TiO_2 films as transparent counter electrodes for electrochromic window" Bull. Korean Chem. Soc. Vol. 19, No. 1, (1998), pp: 107-109.

[7] Divya Haridas, Arijit Chowdhuri, K. Sreenivas, and Vinay Gupta " Enhanced LPG response characteristics of SnO_2 thin film based sensors loaded with Pt clusters" International journal on smart sensing and intelligent systems, Vol. 2, No. 3, (2009), pp: 503-514.

[8] Jeong-Hoon Leea, Gun-Eik Janga, Dae-Ho Yoonb and Sang-Hee Sonc "Effect of deposition temperature on electro-optical properties of SnO_2 thin films fabricated by a PECVD method" Journal of Ceramic Processing Research. Vol. 8, No. 1, (2007), pp: 59-63.

[9] U. Pal, A. Pérez-Centeno, and M. Herrera-Zaldívar "Cathodoluminescence defect characterization of hydrothermally grown SnO_2 nanoparticles" J. Appl. Phys. Vol. 103, No. 064301, (2008), pp: 1-6.

[10] R.G. Dhere, H.R. Moutinho, S. Asher, D. Young, X. Li, R. Ribelin, and T. Gessert" Characterization of SnO_2 Films Prepared Using Tin Tetrachloride and Tetra Methyl Tin Precursors" National Renewable Energy Laboratory, October (1998), pp: 1-6.

[11] D.M. Qu, P.X. Yan, J.B. Chang, D. Yan, J.Z. Liu, G.H. Yue, R.F. Zhuo, H.T. Feng" Nanowires and nanowire–nanosheet junctions of SnO_2 nanostructures" Materials Letters, Vol.61, (2007), pp: 2255–2258.

[12] J. E. Dominguez, X. Q. Pan, L. Fu, P. A. Van Rompay, Z. Zhang, J. A. Nees, and P. P. Pronko, " Epitaxial SnO_2 thin films grown on .1¯ 012. sapphire by femtosecond pulsed laser deposition", J. Appl. Phys., Vol. 91, No. 3, 1 February (2002), pp: 1060-1065.

[13] J. E. Dominguez, L. Fu, and X. Q. Pan "Effect of crystal defects on the electrical properties in epitaxial tin dioxide thin films" Appl. Phys. Lett., Vol. 81, No. 27, 30 December (2002), pp: 5163-5170.

[14] Jochan Joseph, Varghese Mathew, Jacob Mathew, K. E. Abraham " Studies on physical properties and carrier conversion of SnO_2: Nd thin films" Turk J Phys, Vol. 33, (2008), pp: 37-47.

[15] J. Geurts. S. Rau. W. Richter and F. J. Schmitte "SnO films and their oxidation to SnO_2: Raman scattering. IR reflectivity and X-Ray diffraction" Thin Solid Films, (1984).

[16] G. Gordillo; L. C. Moreno; W. De La Cruz; P.Teheran "Preparation and characterization of SnO_2 thin films deposited by spray pyrolysis from $SnCl_2$ and $SnCl_4$ precursors" Thin Solid Films, Vol. 252, No. 1, (1994), pp: 61-66.

[17] Yong-Sahm Choe, Jae-Ho Chung, Dae-Seung Kim, Gyeung-Ho Kim and Hong Koo Baik "Phase transformation and morphological evolution of ion-beam sputtered tin oxide films on silicon substrate" Materials Research Bulletin, Vol. 34, Issue 9, (1999), pp:1473-1479.

[18] Brian S. Mitchell "An introduction to materials engineering and science for chemical and materials engineers" A John Wily & Sons, Inc., Hoboken, New Jersey. All rights reserved. Published simultaneously in Canada, (2004), pp: 43.

[19] S. Mosadegh Sedghi, and M. Vesali Naseh "Sonochemically prepared SnO_2 quantum dots as a selective and low temperature Co sensor" Proceedings of World Academy of Science, Engineering and Technology, Vol. 37, Issue 2070-3740, (2009).

[20] L.V. Azarooff "Elementary of X-Ray Crystallography" Mc Graw-Hill Book Company, (1968), pp: 552-556.

[21] Th. H. De. Keijser, J. Appl. Cryst., Vol.15, (1982), pp: 308-314.

[22] A. Moses Ezhi Raj, L. C. Nehru, M. Jayachandran, and C. Sanjeeviraja "Spray pyrolysis deposition and characterization of highly (100) oriented magnesium oxide thin films" Cryst. Res. Technol.Vol. 42, No.9, (2007), pp: 867 – 875.

[23] A.S. Edelestein, R.C. Camarata "Nanomaterials: Synthesis, Properties and Application, Institute of Physics" Publ., Bristol, UK, (1996).

[24] Ali Jasim AL-Jabiry, " Studying the Effect of Molarity on the Physical and Sensing Properties of Zinc Oxide Thin Films Prepared by Spray Pyrolysis Technique" Phd (University of Technology), (2007), pp: .